Non–conforming sliding interfaces in 3D Finite Element analysis of electrical machines with motion

Enno Lange, François Henrotte and Kay Hameyer
Institute of Electrical Machines – RWTH Aachen University
E–mail: Enno.Lange@IEM.RWTH-Aachen.de

Abstract— **A mapping between the outer surface of the rotor and the inner surface of the stator is a convenient mathematical representation of the relative stator–rotor motion in 2D and 3D electrical machine models. Lagrange multipliers are then used to restore continuity in the weak sense across this non–conforming interface. By choosing biorthogonal nodal shape functions for the Lagrange multipliers in 2D problems, a saddle–point problem can be avoided, i.e. the positive definiteness of the system matrix is preserved. This paper generalizes this result to the nonlinear 3D magnetic vector potential formulation. A class of biorthogonal edge–based shape functions is constructed and implemented resulting in a stable discretization method without remehsing for eddy current 3D problems with motion.**

I. Introduction

STATIC and transient analyses of electrical machines require a flexible variation of the rotor position in the model. An early adopted approach is the moving band (MB) technique [3] whose principle is to re–generate at each time–step a single layer of conforming finite elements in a thin annulus–shaped region of the air gap. However, in practice, air gap re–meshing can be done automatically for 2D rotating machines only. For linear motion in 2D and motion in 3D models, air gap re–meshing would imply invoking a full–fledged automatic mesh generator at each time–step, which is impractical. An hybrid approach by coupling FEM and BEM is chosen within [5] requiring a non CG–solver for a stable solution. The mortar element method (MEM) was proposed in [7] and applied to a 2D machine problem in [1]. The Lagrange multiplier (LM) method has been extensively investigated in [2]. Both MEM and LM can be extended to 3D problems, but the MEM requires an additional integration mesh [8], and for the LM the conditioning worsens significantly [4]. Recently, biorthogonal basis functions for the Lagrange operator known from mechanical stress analysis [9] have been successfully adopted to a 2D quasi–static magnetic vector potential formulation [6] preserving the symmetry and positive definiteness of the equation system. An extension to 3D problems is described in this paper.

II. Variational Formulation

Let Ω^m and Ω^s be the master and the slave domain respectively, e.g. the stator and rotor of an electric machine. Let $\Gamma^m \subset \partial\Omega^m$ and $\Gamma^s \subset \partial\Omega^s$ be the sliding interface between the master and the slave domain and $p : \Gamma^s \rightarrow \Gamma^m$ be a smooth mapping that may account for a relative motion between the stator and the rotor.

Assuming for the sake of simplicity homogeneous Dirichlet boundary conditions on $\partial\Omega^m \setminus \Gamma^m \cup \partial\Omega^s \setminus \Gamma^s$ (Neumann boundary conditions would be treated in the classical way), the variational calculus applied to the energy balance of the system leads to the weak formulation, i.e. the equation

$$\sum_{k=m,s} \int_{\Omega^k} \left(\mathbf{H}^k \operatorname{curl} \delta\mathbf{A}^k - \mathbf{J}^k \delta\mathbf{A}^k \right) \mathrm{d}\Omega^k + \int_{\Gamma^s} \left\{ \delta\boldsymbol{\lambda} \left(\mathbf{A}^s - \mathbf{A}^m \circ p \right) + \boldsymbol{\lambda} \left(\delta\mathbf{A}^s - \delta\mathbf{A}^m \circ p \right) \right\} \mathrm{d}\Gamma^s = 0, \tag{1}$$

which must be verified for arbitrary variations $\delta\mathbf{A}^k$ and $\delta\boldsymbol{\lambda}$ of the magnetic vector potential $\mathbf{A}^k$ on the domain $k = m, s$ and of the Lagrange multiplier $\boldsymbol{\lambda}$ that fulfill the boundary conditions. The magnetic field ist described by $\mathbf{H}^k$ and the current density is given by $\mathbf{J}^k$.

III. Discretization

Following the usual discretization approach, the magnetic vector potential and the Lagrange multiplier are approximated by

$$\mathbf{A}^k = \sum_l A_l^k \boldsymbol{\alpha}_l^k, \qquad \delta\mathbf{A}^k = \{\boldsymbol{\alpha}_l^k\}, \tag{2}$$

$$\boldsymbol{\lambda} = \sum_j \lambda_j \boldsymbol{\mu}_j, \qquad \delta\boldsymbol{\lambda} = \{\boldsymbol{\mu}_j\}, \tag{3}$$

with the functional spaces being spanned by the edge shape functions $\boldsymbol{\alpha}_l^k$ and $\boldsymbol{\mu}_j$. From the weak formulation (1) one obtains the saddle point problem:

$$\begin{pmatrix} \mathbf{S}_{i,i}^m & \mathbf{S}_{i,\Gamma}^m & 0 & 0 & 0 \\ \mathbf{S}_{\Gamma,i}^m & \mathbf{S}_{\Gamma,\Gamma}^m & 0 & 0 & -\mathbf{M}^T \\ 0 & 0 & \mathbf{S}_{\Gamma,\Gamma}^s & \mathbf{S}_{\Gamma,i}^s & \mathbf{D}^T \\ 0 & 0 & \mathbf{S}_{i,\Gamma}^s & \mathbf{S}_{i,i}^s & 0 \\ 0 & -\mathbf{M} & \mathbf{D} & 0 & 0 \end{pmatrix} \begin{pmatrix} \mathbf{A}_i^m \\ \mathbf{A}_\Gamma^m \\ \mathbf{A}_\Gamma^s \\ \mathbf{A}_i^s \\ \boldsymbol{\lambda} \end{pmatrix} = \begin{pmatrix} \mathbf{b}^m \\ 0 \\ 0 \\ \mathbf{b}^s \\ 0 \end{pmatrix}. \tag{4}$$

Within (4) the standard stiffness matrix is denoted by $\mathbf{S}^k$. The circulations of the vector potential along edges belonging to the surface Γ are noted $\mathbf{A}_\Gamma^k$, whereas those along internal edges

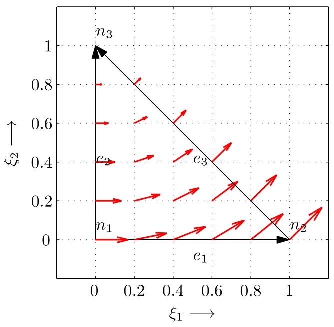

Fig. 1. Standard shape function $\boldsymbol{\alpha}_1$.

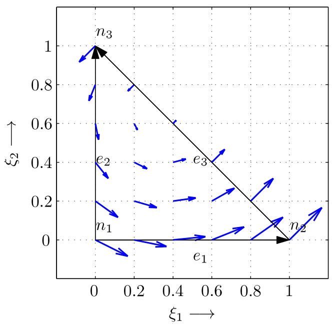

Fig. 2. Biorthog. shape function $\boldsymbol{\mu}_1$.

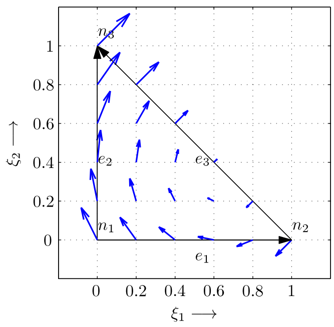

Fig. 3. Biorthog. shape function $\boldsymbol{\mu}_2$.

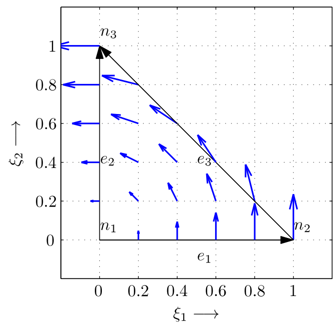

Fig. 4. Biorthog. shape function $\boldsymbol{\mu}_3$.

are noted $\mathbf{A}_i^k, k = m, s$. The coupling matrices in (4) are constructed according to:

$$D_{jl} = \int_{\Gamma^s} \boldsymbol{\mu}_j \boldsymbol{\alpha}_l^s \, \mathrm{d}\Gamma^s, \tag{5}$$

$$M_{jl} = \int_{\Gamma^s} \boldsymbol{\mu}_j \boldsymbol{\alpha}_l^m \circ p \, \mathrm{d}\Gamma^s. \tag{6}$$

The last line of (4) can be re–written

$$\mathbf{A}_\Gamma^s = \mathbf{Q}\mathbf{A}_\Gamma^m \quad \text{with} \quad \mathbf{Q} =: \mathbf{D}^{-1}\mathbf{M} \equiv \left(\mathbf{M}^T\mathbf{D}^{-T}\right)^T \tag{7}$$

so that the Lagrange multiplier $\boldsymbol{\lambda}$ can be eliminated:

$$\begin{pmatrix} \mathbf{S}_{i,i}^m & \mathbf{S}_{i,\Gamma}^m & 0 \\ \mathbf{S}_{\Gamma,i}^m & \mathbf{S}_{\Gamma,\Gamma}^m + \mathbf{Q}^T\mathbf{S}_{\Gamma,\Gamma}^s\mathbf{Q} & \mathbf{Q}^T\mathbf{S}_{\Gamma,i}^s \\ 0 & \mathbf{S}_{i,\Gamma}^s\mathbf{Q} & \mathbf{S}_{i,i}^s \end{pmatrix} \begin{pmatrix} \mathbf{A}^m \\ \mathbf{A}_\Gamma^m \\ \mathbf{A}^s \end{pmatrix} = \begin{pmatrix} \mathbf{b}^m \\ 0 \\ \mathbf{b}^s \end{pmatrix}. \tag{8}$$

The reduced system matrix is symmetric and positive definite. However, according to the properties of $\mathbf{D}$, the inversion in (7) can be a computationally expansive or not.

IV. Biorthogonal shape functions

Each time the mapping p changes, the inversion of $\mathbf{D}$ must be performed. A diagonalization of $\mathbf{D}$ allows for an inversion during the element–wise assembly of the system matrix and can be achieved be choosing the basis functions $\boldsymbol{\mu}$ of $\boldsymbol{\lambda}$ in a dual function space, similar to [9] and extended to edge based shape functions, yielding a biorthogonality condition:

$$D_{jl} = \int_{\Gamma^s} \boldsymbol{\mu}_j \boldsymbol{\alpha}_l^s \, \mathrm{d}\Gamma^s = \delta_{jl} \int_{\Gamma^s} |\boldsymbol{\alpha}_l^s| \, \mathrm{d}\Gamma^s, \quad \delta_{jl} = \begin{cases} 1, \text{ if } j = l \\ 0, \text{ if } j \neq l. \end{cases} \tag{9}$$

The edge shape functions $\boldsymbol{\varphi}_l = \{\boldsymbol{\alpha}_l, \boldsymbol{\mu}_l\}$ of the edge e_l between the vertices n_r and n_s are constructed according to the standard approach

$$\boldsymbol{\varphi}_l = \varphi_r \,\mathrm{grad}\, \varphi_s - \varphi_s \,\mathrm{grad}\, \varphi_r \tag{10}$$

with the nodal shape function $\varphi_g = \{\alpha_g, \mu_g\}$ of vertex n_g. Here, α_g are the standard nodal shape function whereas (9) yields a system of equations for the polynomial coefficients of the nodal shape functions μ_g:

$$\begin{pmatrix} \mu_1 \\ \mu_2 \\ \mu_3 \end{pmatrix} = \begin{pmatrix} -a & -a \\ b & -\frac{b}{2} \\ -\frac{b}{2} & b \end{pmatrix} \begin{pmatrix} \xi_1 \\ \xi_2 \end{pmatrix} + \begin{pmatrix} a \\ 0 \\ 0 \end{pmatrix}, \tag{11}$$
$$a := 1.040264466, \quad b := 1.471156117.$$

The biorthogonal edge shape functions $\boldsymbol{\mu}_l$ are then built by (10). The standard edge based shape function $\boldsymbol{\alpha}_1$ of the reference triangle in barycentric coordinates ξ_1 and ξ_2 is shown in Fig. 1 and the corresponding biorthogonal shape function $\boldsymbol{\mu}_1$ is depicted in Fig. 2. For the sake of completeness the biorthogonal edge shape functions $\boldsymbol{\mu}_2$ and $\boldsymbol{\mu}_3$ are shown in Fig. 3 and Fig. 4 respectively.

V. Discussion and Conclusions

The proposed biorthogonal edge shape functions ensure the continuity of the magnetic vector potential in the weak sense across a non–conforming interface i.e. the sliding interface between stator and rotor in the 3D FE analysis of e.g. electric machines. Furthermore, this approach allows for a consistent implementation in 2D and 3D, both for translational and rotational motion modelling. Numerical stability is preserved thanks to the symmetry and the positive definiteness of the resulting system matrix. A detailed elaboration of the proposed approach along with the application to TEAM–problems and a rotating machine will be given in the full paper.

References

[1] O. Antunes, J. Bastos, N. Sadowski, A. Razek, L. Santandrea, F. Bouillault, and F. Rapetti. Using hierarchic interpolation with mortar element method for electrical machines analysis. *Magnetics, IEEE Transactions on*, 41(5):1472–1475, 2005.

[2] O. Antunes, J. Bastos, N. Sadowski, A. Razek, L. Santandrea, F. Bouillault, and F. Rapetti. Torque calculation with conforming and non-conforming movement interface. *Magnetics, IEEE Transactions on*, 42(4):983–986, 2006.

[3] B. Davat, Z. Ren, and M. Lajoie-Mazenc. The movement in field modeling. *Magnetics, IEEE Transactions on*, 21(6):2296–2298, 1985.

[4] C. Golovanov, J. Coulomb, Y. Marechal, and G. Meunier. 3D mesh connection techniques applied to movement simulation. *Magnetics, IEEE Transactions on*, 34(5):3359–3362, 1998.

[5] S. Kurz, J. Fetzer, G. Lehner, and W. Rucker. A novel formulation for 3D eddy current problems with moving bodies using a lagrangian description and BEM-FEM coupling. *Magnetics, IEEE Transactions on*, 34(5):3068–3073, 1998.

[6] E. Lange, F. Henrotte, and K. Hameyer. A variational formulation for nonconforming sliding interfaces in finite element analysis of electric machines. *Magnetics, IEEE Transactions on*, 46(8):2755–2758, 2010.

[7] F. Rapetti, E. Bouillault, L. Santandrea, A. Buffa, Y. Maday, and A. Razek. Calculation of eddy currents with edge elements on non-matching grids in moving structures. *Magnetics, IEEE Transactions on*, 36(4):1351–1355, 2000.

[8] F. Rapetti, Y. Maday, F. Bouillault, and A. Razek. Eddy-current calculations in three-dimensional moving structures. *Magnetics, IEEE Transactions on*, 38(2):613–616, 2002.

[9] B. I. Wohlmuth. A mortar finite element method using dual spaces for the lagrange multiplier. *SIAM Journal on Numerical Analysis*, 38(3):989–1012, 2001.